


Correlation of Wall Microstructure and Heterogeneous Distributions of Strain in Evolving Murine Abdominal Aortic Aneurysms

JOHN S. WILSON ^{1,4} MATTHEW R. BERSI,¹ GUANGXIN LI,² and JAY D. HUMPHREY^{1,3}

¹Department of Biomedical Engineering, Yale University, New Haven, CT, USA; ²Department of Surgery, Yale School of Medicine, New Haven, CT, USA; ³Vascular Biology and Therapeutics Program, Yale School of Medicine, New Haven, CT, USA; and ⁴Department of Radiology, Emory University, Atlanta, GA, USA

(Received 7 October 2016; accepted 20 March 2017; published online 4 April 2017)

Associate Editor Ajit P. Yoganathan oversaw the review of this article.

Abstract—A primary deficiency in predicting the progression and rupture-risk of abdominal aortic aneurysms (AAAs) is an inability to assign patient-specific, heterogeneous biomechanical properties to the remodelling aortic wall. Toward this end, we investigated possible correlations between three quantities having the potential for non-invasive measurement (diameter, wall thickness, and strain) and local wall microstructure within evolving experimental AAAs. AAAs were initiated in male C57BL/6J mice *via in situ* adventitial application of elastase and allowed to progress for 1–4 weeks. Regional *in vitro* Green strain was assessed using custom panoramic digital image correlation and compared to local geometry and histology. Diameter correlated mildly with elastin grade and collagen, when considering all circumferential locations and remodeling times. Normalized wall thickness correlated strongly with normalized collagen area fraction, though with outliers in highly cellular regions. Circumferential Green strain correlated strongly with elastin grade when measured over the range of 20–140 mmHg, though the correlation weakened across a physiologic range of 80–120 mmHg. Axial strain correlated strongly between *in vitro* and physiologic ranges of pressures. Circumferential heterogeneities render diameter a poor predictor of underlying regional microstructure. Thickness may indicate collagen content, though corrections are needed in regions of increased cellularity. *In vitro* circumferential strain predicts local functional elastin over large ranges of pressure, but there is a need to extend this correlation to clinically relevant pressures. Axial strain in the aneurysmal shoulder region may reflect the elastic integrity within the apical region of the lesion and should be explored as an indicator of disease severity.

Keywords—Biomechanics, Elastase, Regional heterogeneity, Panoramic digital image correlation.

INTRODUCTION

Abdominal aortic aneurysms (AAAs) continue to be a significant cause of morbidity, mortality, and medical expense in older populations. The most serious consequence of AAAs is rupture, which can carry mortality rates as high as 90%.¹ Since rupture likely depends on local, not just global, biological and mechanical properties, significant challenges remain in accurately assessing rupture risk on a patient-specific basis because of the spatially varying properties across a complex geometry.

Prior assessments of regional properties have focused primarily on excising samples from an AAA at multiple locations and conducting biological (e.g., gene expression or protease activity), structural (e.g., elastin degradation or collagen fiber density and orientation), or mechanical (e.g., stress–strain) tests. Such studies are necessarily limited to the few regions from which the samples come. Additionally, relatively large samples are required for mechanical testing, which yield spatially averaged quantities. Excision also alters the native geometry of the vessel, which may influence the measured mechanical behavior (e.g., *via* the release of residual stress). Since controlled tests on AAA progression require animal models (often rodents), there is also a need for methods that can quantify regional biomechanical properties on small (often sub-millimeter) scales. Development of a small scale panoramic digital image correlation (pDIC) mechanical testing system thus represents a promising advance.^{8,9} Allowing a full-field assessment of strain on the surface of an excised, pressurized, and axially extended murine specimen, pDIC has been used successfully to study aortas from both acute elastase perfusion and chronic angiotensin infusion induced aneurysms in mice.^{7,10}

Address correspondence to John S. Wilson, Department of Radiology, Emory University, Atlanta, GA, USA. Electronic mail: john.s.wilson@emory.edu

The present study focuses on another murine model of AAA and uses pDIC to investigate the potential of estimating regionally heterogeneous biomechanical properties, which inherently depend on the local underlying microstructure, by correlating elastin and collagen content with three non-invasively measurable quantities: diameter, wall thickness, and mechanical strain. We emphasize that we do not seek to study the evolution of a particular murine model of AAA *per se*, but rather to utilize the model to create a diverse set of heterogeneous AAA samples with different extents of remodeling to test potentially predictive correlations of mechanical strain and evolving microstructure. Such correlations, if established, may provide increased insight into the evolving biomechanical properties of AAAs as well as aid in the development of patient-specific computational models of AAA progression and rupture-risk for which *in vitro* correlates of structure and properties are not feasible.

METHODS

Adventitial Elastase Model of AAAs

A modified version of an adventitially applied elastase model of AAAs was used.⁴ Briefly, 9 male, C57BL/6J mice (age 14–17 weeks) underwent survival surgery under isoflurane anesthesia to expose the anterior surface of the infrarenal abdominal aorta by gentle dissection. Sterile porcine pancreatic elastase in normal saline (~8 μ L at 10 U/mL, Sigma E7885) was applied onto a 1x4 mm strip of sterile gauze and placed atop the adventitial aortic surface for 10 min. After removing the gauze, the peritoneal space was lavaged three times with 0.5 mL of sterile normal saline. Three additional mice (age 17–21 weeks) did not undergo surgery and served as true controls since the goal of the surgery was to create a diverse set of heterogeneously evolving lesions. All surgeries and post-operative care were approved by and performed according to the policies of the Yale Institutional Animal Care and Use Committee.

Mechanical Testing

Mice were euthanized *via* intraperitoneal injection of Beuthanasia-D (150 mg/kg), the infrarenal aorta was exposed, and black India ink dots were applied on its anterior surface to measure the *in situ* length and to aid in anatomical orientation. Excised vessels from control (0 week) and post-operative (1, 2, or 4 week) animals were carefully dissected free of surrounding tissue and side branches were ligated with 9-0 suture. The *in vitro* axial length was measured and *in vivo* axial stretch was estimated (i.e., ratio of *in situ* to *in vitro*

axial length) using the superficial India ink dots as fiducial markers. The sample was then cannulated and restored to its *in vivo* axial length prior to the application of a random speckle pattern to the outer adventitial surface using an airbrush to spray black and white waterproof India ink.

Mechanical tests using a custom pDIC system were performed as described previously.^{7–10} Specimens were mounted co-axially within a 45° concave conical mirror, distended with Hank's balanced salt solution (Gibco 14025-092) using a computer controlled syringe pump, and imaged from 8 symmetric perspectives by a rotating overhead camera fixed at a small stereo angle (<1°) relative to the central axis of the mirror. This procedure was repeated at pressures ranging from 0 to 140 mmHg, in increments of 10 mmHg. Post-processing and analysis of the acquired pDIC images was performed in Matlab (Mathworks) and Rhinoceros 3D (Robert McNeel & Associates) using custom scripts. Briefly, each symmetric image was unwrapped using a polar to Cartesian coordinate transformation. Small regions (templates) defined in the unwrapped reference configuration (e.g., *in vivo* stretch and 70 mmHg) were tracked through all deformed configurations by comparison with a larger (analysis) region in each subsequent image. Normalized cross-correlation coefficients (NCC) were computed based on regional grayscale intensities in the corresponding template and analysis windows with areas of 21 × 21 and 41 × 41 pixels, respectively. Unwrapping increases correlation accuracy by transforming template rotations into translations, and the known coordinate transformation allows tracked points to be re-wrapped prior to reconstruction. The outer surface of the conical mirror was marked with a pre-defined calibration target. Each symmetric image was individually calibrated using the direct linear transformation (DLT) method to identify the position of the corresponding virtual camera and hence the spatial coordinates of the calibration target in the global reference system. Taking advantage of the known geometry of the concave conical mirror, a ray-tracing procedure was used to reconstruct the position of the tracked points on the surface of the sample. Points reconstructed from multiple symmetric stereo views were merged to overcome reconstruction errors at the stereo plane, thus allowing an accurate full field surface reconstruction. Raw full field displacements were computed by subtracting the reconstructed coordinates in the deformed configurations from the reconstructed coordinates in the reference configuration. Once identified, each component of the reconstructed displacement field was smoothed using a NURBS-based parametric surface fitting and subsequently added back to the reference configuration to yield the final smoothed deformed geometries. Tracked

points were then triangulated and element connectivity was maintained throughout all deformations. Thus, element-wise finite strains were directly computed between pressurization states. Namely, the local 2D deformation gradient tensor was estimated from the position vectors of two sides of each triangular domain in the reference and deformed configuration, ultimately allowing the calculation of the 2D Green strain tensor. Further details on the pDIC system, calibration, and analysis can be found elsewhere.^{2,6,8–10}

Histology and Correlations

After testing, each sample was loaded to its *in vivo* axial length and pressure of 20 mmHg and fixed overnight in 10% formalin. Using the reconstructed 3D pDIC geometry, axial locations of the proximal shoulder and apex of each lesion were identified and recorded. Following standard preparation of paraffin embedded samples, corresponding cross-sections of the preserved sample for each region were stained with Masson's trichrome (MTC) and Movat's pentachrome (MVT) for collagen and elastin, respectively. Images were captured using an Olympus BX51 microscope at $\times 20$ magnification. Anterior (determined by the location of elastolytic damage) and posterior regions at the shoulder and apex were selected and analyzed, unless they did not demonstrate adequate histological quality for quantitative analysis (e.g., due to sectioning artifacts within the heterogeneously remodeled wall). Overall, 31 samples from 12 aortas [control ($n = 3$), 1 week ($n = 4$), 2 weeks ($n = 2$), and 4 weeks ($n = 3$)] were analyzed. Samples at 2 and 4 weeks were similar and thus grouped for analysis. Separate anterior and posterior regions were not identified for control samples as there was no damage; instead, results from two cross-sections per aorta were averaged to give final homogeneous values. Average wall thickness for each region was calculated using ImageJ (NIH) as the mean of at least 8 measurements per image. Thickness was normalized using the average value from all control samples. Similarly, the non-fixed pressurized outer diameters (at 140 mmHg) were quantified at each axial location from the pDIC data using Rhinoceros 3D and normalized using the average diameter of the controls.

Collagen area fraction was quantified similar to prior reports.³ Briefly, custom colorimetric analysis allowed blue pixels to be extracted from selected regions in MTC stained slides (one per region), and an area fraction was calculated relative to the total cross-sectional area (see Fig. 1). Relative collagen content per region was calculated by multiplying the area fraction by the average local wall thickness. Finally, normalized collagen content per region was calculated by dividing the relative collagen content by the average

relative collagen content from control samples. Functional elastin was determined from MVT stained slides by a single investigator using a semi-quantitative grade ranging from 0 to 4 defined as the average number of elastic lamellae in a region of interest minus one grade point for signs of damage (e.g., elastin fragmentation, thinning lamellae, or changes in smooth muscle cell (SMC) shape or area) (Fig. 2). Adventitial cellularity was also semi-quantitatively graded by a single investigator on a 0 to 4 scale, where 0 represents rare cells (control), 1 a mild increase, 2 a moderate increase confined mainly to the inner adventitia, 3 a moderate increase throughout the adventitia, and 4 a marked increase throughout the adventitia (Fig. 2).

The previously recorded axial locations corresponding to the analyzed histological cross-sections (shoulder and apex) were transferred to the reconstructed meshed 3D geometry using ParaView (Kitware), and square patches having a width approximately one-sixth of the local circumference were selected along the anterior and posterior sides (Fig. 1). The mean circumferential and axial Green strains for all elements included in each patch were calculated for correlation with regional histology. General correlation between two variables was quantified with either a Pearson (ρ_p) or Spearman's rank (ρ_s) correlation coefficient, the latter for semi-quantitative pathology grades. Statistical comparison between the means of three or more groups was performed using either one-way ANOVA with post hoc Bonferroni correction or the non-parametric Kruskal–Wallis test (for pathology grades). Significance was defined as $p < 0.05$.

RESULTS

Elastase produced a mean dilation of $137 \pm 8\%$ at the apex after 1 week and $162 \pm 14\%$ after 2–4 weeks, relative to control ($p < 0.001$, Fig. 3a). As expected, dilatations were primarily anterior and there were no ruptures. Excision of the AAAs revealed an asymmetric axial retraction, with posterior bending due to greater elastic recoil of the untreated posterior wall. Qualitative histological examination revealed marked elastolysis at the anterior apex, with a lesser degree at the anterior shoulder. In general, normalized collagen was greater at the anterior wall of the apex than at the posterior wall; elastin grade and circumferential Green strain were lower, however. When comparing stages of lesion progression at the anterior apex, increased remodeling time led to significantly increased diameter, wall thickness, and normalized collagen with associated decreases in elastin grade and circumferential strain (Figs. 3a–3e). Adventitial cellularity increased

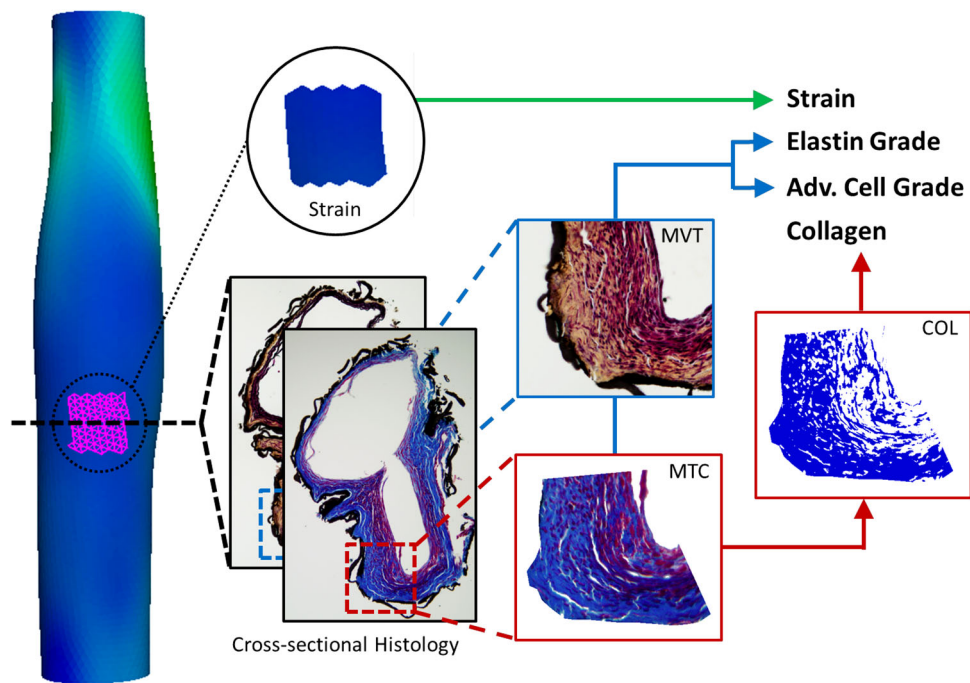


FIGURE 1. Schema of regional correlations of biaxial strain and key histological features (elastin grade, adventitial cell grade, and collagen). MVT—Movat's Pentachrome, MTC—Masson's trichrome, COL—extracted collagen area. Such correlations were repeated across multiple regions.

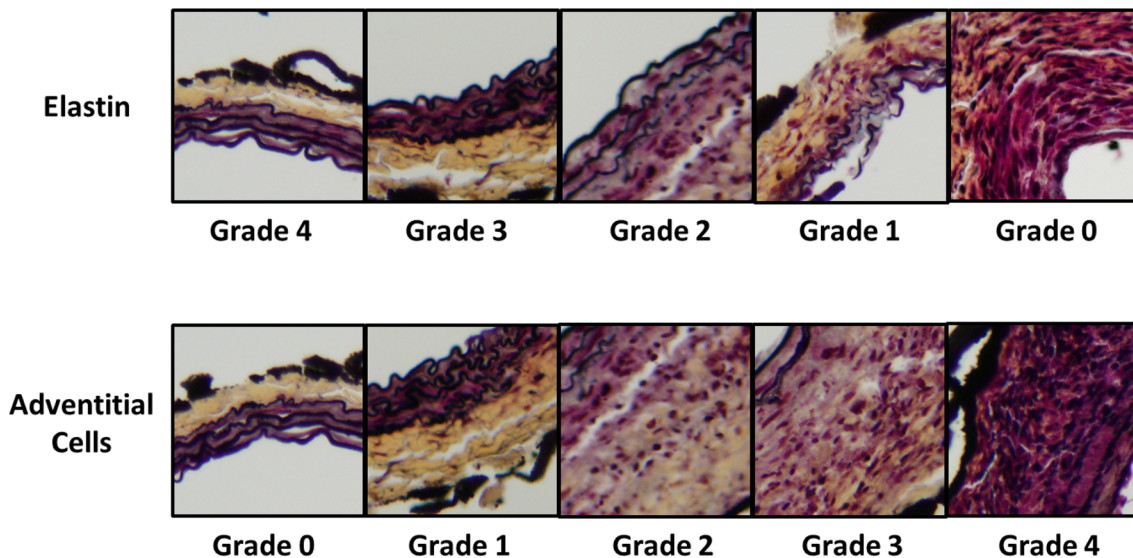


FIGURE 2. (Top) Elastin grades based on the number of elastic lamellae and damage. (Bottom) Grades of adventitial cellularity based on severity and distribution. (20x).

significantly at 1 week, then decreased on average even though the decline did not reach statistical significance (Fig. 3f). Thickness and elastin grade at the anterior apex were not correlated significantly.

An illustrative full-field reconstruction of the circumferential Green strain (between 20 and 140 mmHg) is shown in Fig. 4 for one AAA. Note the heterogeneous strain field: low values along the anterior bulge,

consistent with elastolysis and preservation or increase of collagen, but higher values in the untreated posterior regions of the lesion. Low strains at the proximal neck were likely secondary to its proximity to the suture securing the sample to the cannula. Axial strains were much lower than circumferential strains due to testing at a fixed axial stretch. While full biaxial testing is useful for a more complete mechanical analysis of a

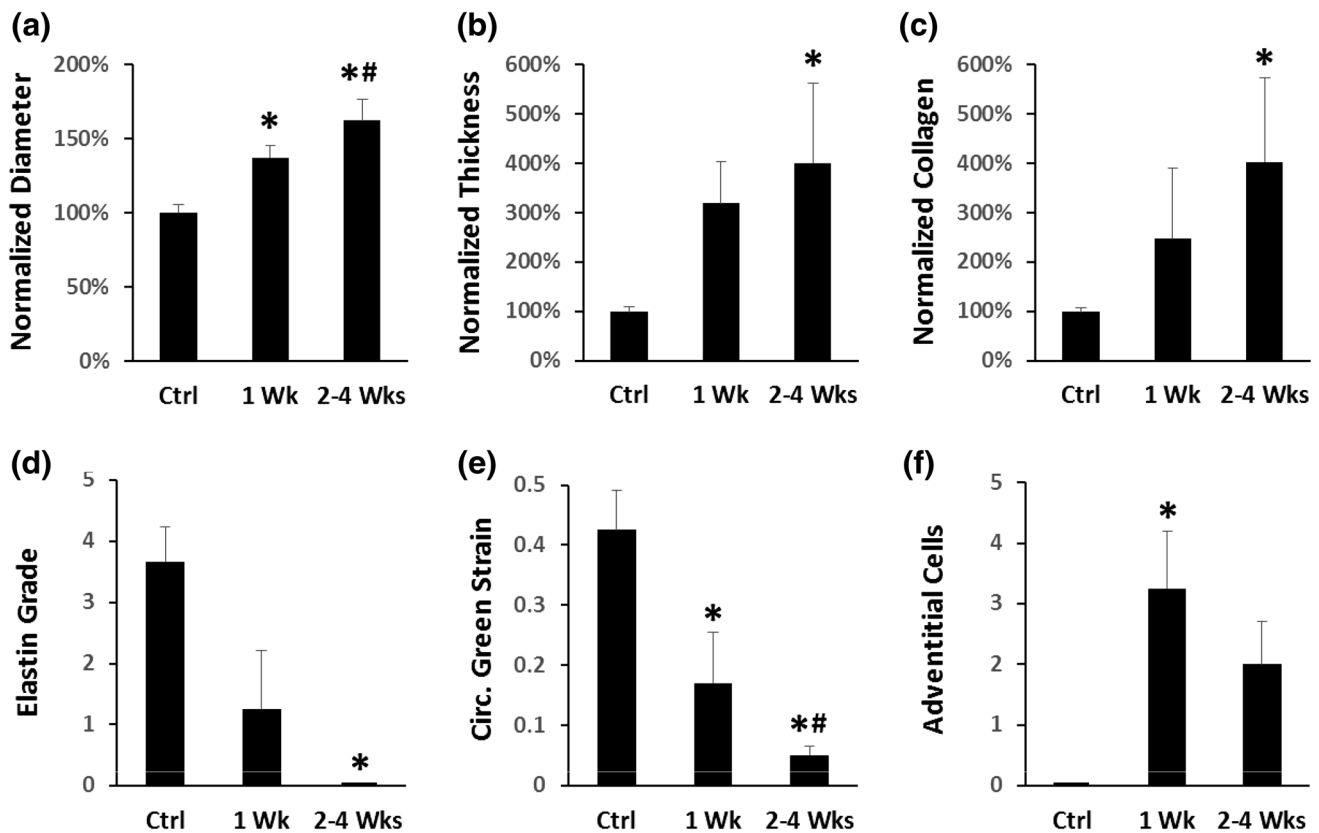


FIGURE 3. Comparisons of mean \pm SD normalized diameter (a), normalized thickness (b), normalized collagen (c), elastin grade (d), circumferential Green strain (20–140 mmHg) (e), and adventitial cell grade (f) at the anterior apex as a function of time since elastase application. (* $p < 0.05$ compared to control; # $p < 0.05$ compared to 1 week).

tissue, inflation testing at a fixed axial length mimics the natural loads experienced *in vivo*.

To create a biomechanically diverse data set from which to identify potential general constitutive relationships for any location or state of remodeling, regional Green strain (20–140 mmHg), diameter, wall thickness, and corresponding histological measurements of elastin and collagen were compared using data from up to four locations (anterior and posterior apex and shoulder) per aneurysm. For this complete data set including all locations, remodeling times, and controls, normalized collagen and normalized wall thickness appeared strongly and directly correlated ($\rho_P = 0.94$, $p < 0.001$) (Fig. 5), except for a few potential outliers in regions with high cellularity. Normalized collagen and elastin grade were not well correlated, though the limited 4-week data suggested that this correlation may improve over time following growth and remodeling of collagen. Cross-sectional diameter correlated mildly negatively to elastin grade ($\rho_S = -0.51$, $p < 0.005$) and positively to collagen ($\rho_P = 0.60$, $p < 0.001$) (Fig. 6).

Notably, elastin grade demonstrated a strong, linear correlation with circumferential Green strain

($\rho_S = 0.96$, $p < 0.001$) (Fig. 7). Significant differences were found between the means of all groups except grades 2 and 3 ($p < 0.001$). Scatter plots of circumferential Green strain and elastin suggested a generally decreased strain (and elastin grade) for regions anterior vs. posterior and for increased remodeling time. While increased normalized collagen generally reflected lower circumferential Green strain, clinically useful correlations were poor due to the wide variation in strain from samples having normal collagen content (Fig. 8). Axial Green strains did not correlate predictively with local elastin or collagen content when considering all locations and remodeling times (not shown).

While *in vitro* analysis of strain with pDIC allows a survey over a broad range of pressures, clinical estimates of strain using non-invasive imaging will be restricted to physiologic pressures. Thus, Green strains were compared between 80 and 120 mmHg and 20–140 mmHg, noting that one outlier was removed for the circumferential strain comparison as determined by its Mahalanobis distance being 4.6 standard deviations from the mean (with the next greatest distance being 0.69σ). Circumferential strain correlated mildly

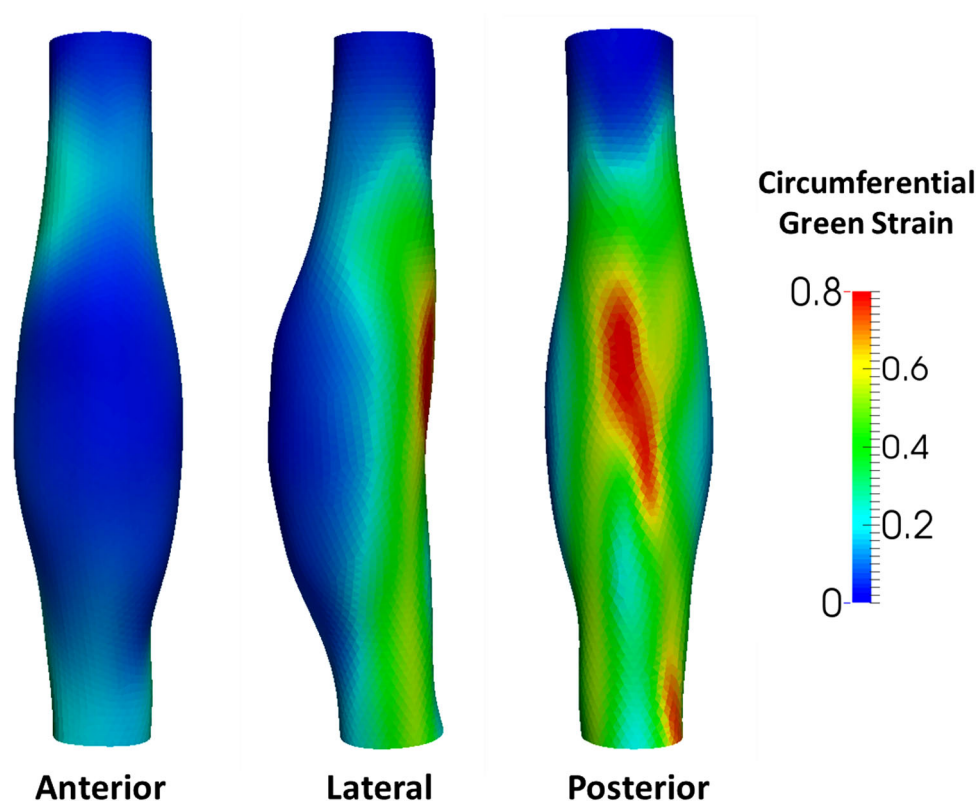


FIGURE 4. Circumferential Green strain field (three views) for a small abdominal aortic aneurysm 4 weeks after elastase application to the anterior adventitial surface, as measured by pressurizing from 20 mmHg to 140 mmHg.

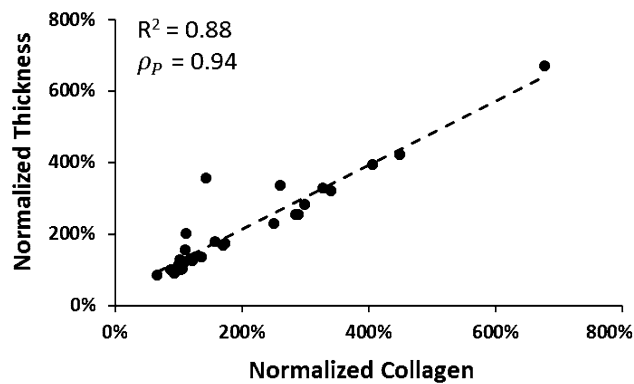


FIGURE 5. Thickness as a function of collagen for all samples, as measured in terms of extracted area fraction of collagen from MTC staining and normalized as a percent relative to control samples. Note the strong, direct correlation ($\rho_p = 0.94$).

between physiologic and *in vitro* ranges ($\rho_p = 0.66$, $p < 0.001$), though not with high fidelity (Fig. 9, left). Indeed, the strong correlation between elastin grade and *in vitro* circumferential strain was lessened when assessed over physiologic pressures ($\rho_s = 0.69$, $p < 0.001$) (Fig. 9, right). On the other hand, axial strain appeared to correlate strongly between the *in vitro* and physiologic ranges ($\rho_p = 0.93$, $p < 0.001$), though the values were an order of magnitude lower (Fig. 10).

DISCUSSION

Need for Heterogeneous Characterization of Microstructure

Despite advances in medical imaging and surgical approach, treatment of AAAs remains a challenge primarily because of the inability to predict which lesions are mechanobiologically stable and which require prompt intervention. Mechanical models that estimate wall stress are promising since rupture is

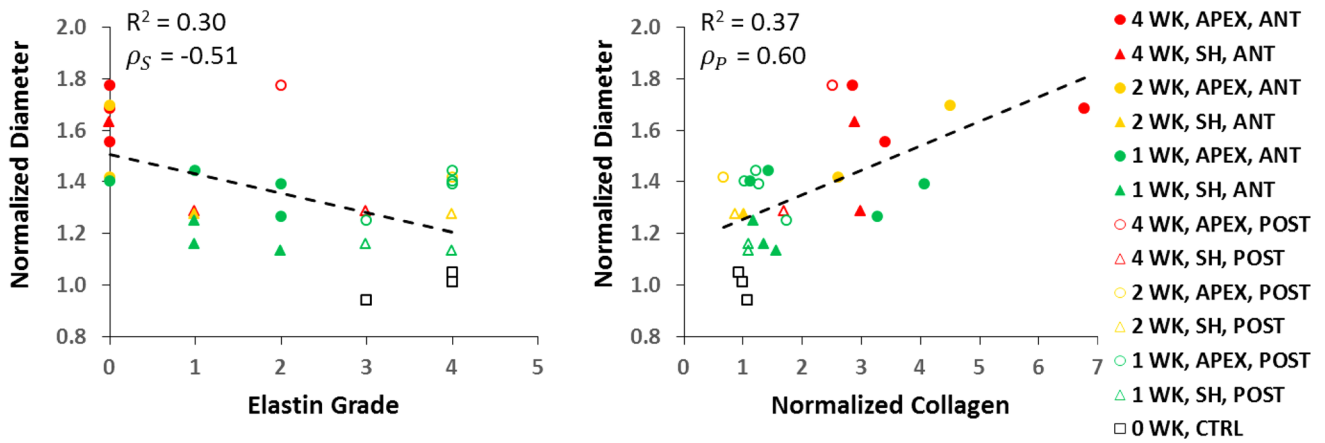


FIGURE 6. Normalized diameter as a function of elastin grade (left) and normalized collagen (right) for each region (APEX vs. shoulder – SH; anterior – ANT vs. posterior - POST) and remodeling time (0-4 wks).

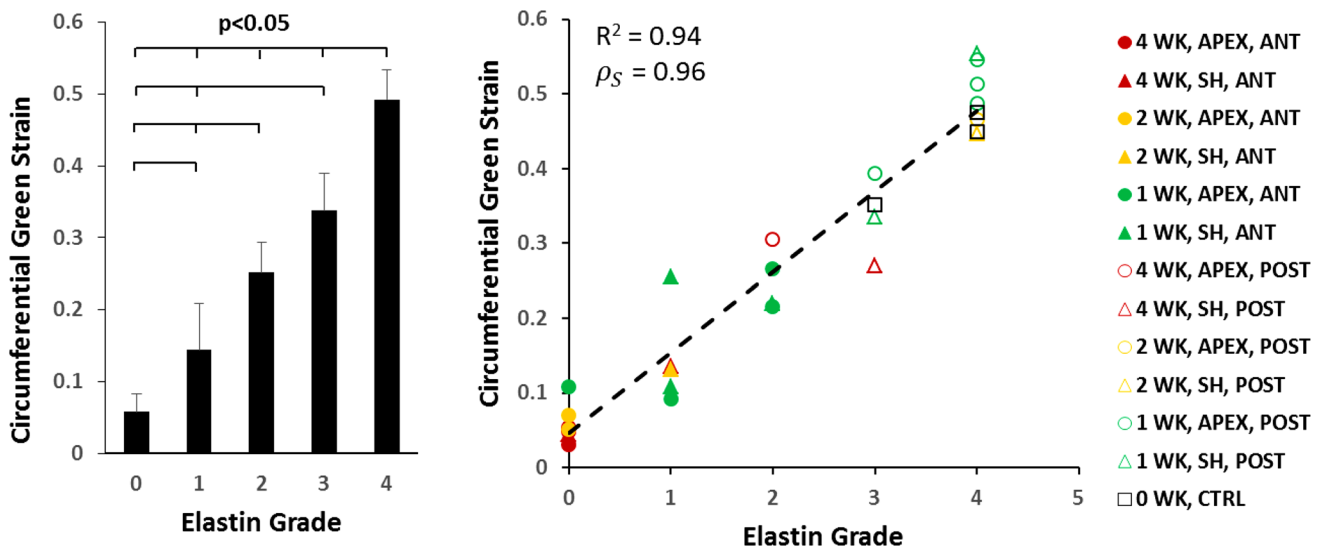


FIGURE 7. (Left) Mean \pm SD circumferential Green strain (20-140 mmHg) as a function of elastin grade. Averages were significantly different among all groups, except between grades 2 and 3. (Right) Scatter plot of circumferential Green strain vs. elastin grade separately for each region (APEX vs. shoulder - SH) and remodeling time (0-4 wks). Note the strong linear relationship ($\rho_S = 0.96$), with generally lower strains with increasing remodeling time and anterior (ANT) rather than posterior (POST) location.

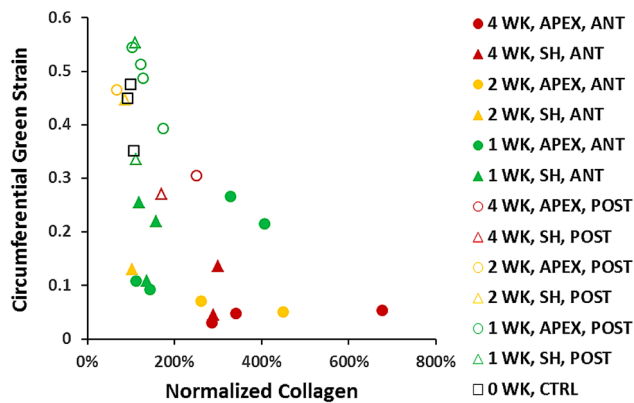


FIGURE 8. Circumferential Green strain (20-140 mmHg) as a function of normalized collagen at each region and remodeling time.

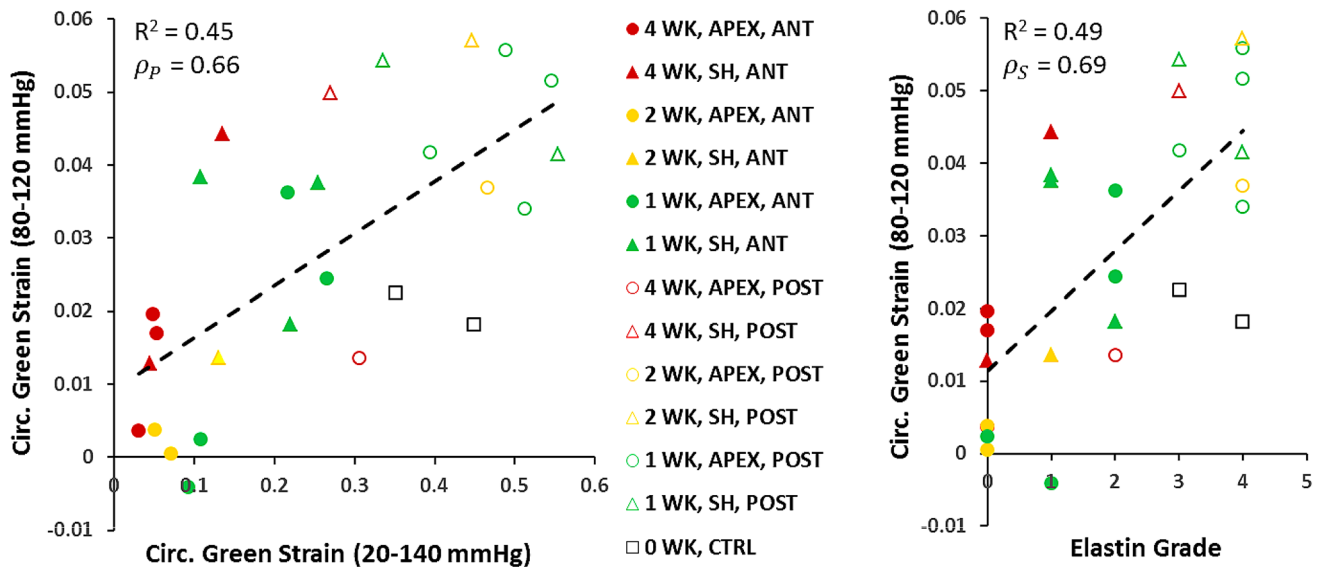


FIGURE 9. (Left) Physiologic circumferential Green strain (80-120 mmHg) as a function of *in vitro* circumferential Green strain (20-140 mmHg). (Right) Physiologic circumferential Green strain (80-120 mmHg) as a function of elastin grade.

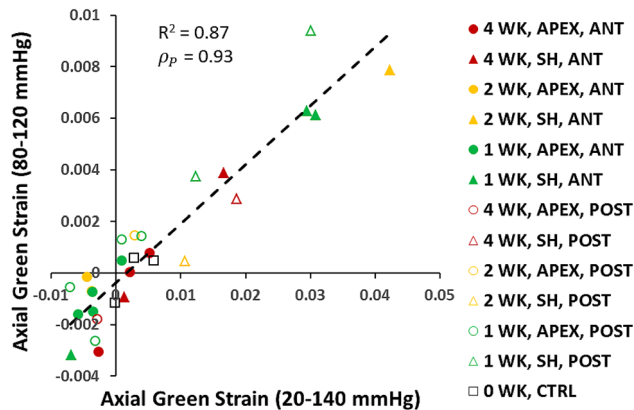


FIGURE 10. Physiologic axial Green strain (80-120 mmHg) as a function of *in vitro* axial Green strain (20-140 mmHg). Note the strong linear correlation ($\rho_p = 0.93$) and that the eight largest axial strains are from shoulder regions.

ultimately a mechanical failure that occurs when wall stress exceeds strength. Yet, neither stress nor strength can be measured directly. Rather, stress must be computed either from geometry, material properties, and applied loads or simply from strain and material properties. Although these properties should be assigned spatially over the lesion, many prior computational models have assumed static material homogeneity (i.e., constant properties) despite evidence to the contrary.^{18,20,21} Because diameter, wall thickness, and strain can potentially be measured noninvasively, we sought possible correlations of these patient-specific, spatially heterogeneous metrics with underlying load-bearing components of the aneurysmal wall that ultimately determine its local mechanical properties. Indeed, many current growth and remodeling models of AAA progression aim to capture the

heterogeneous evolution of these primary load-bearing components (e.g., collagen and elastin), and thus would benefit greatly from non-invasive inference of microstructure for validation and refinement. The adventitious murine elastase model was chosen since it yields non-dissecting, heterogeneous dilatations both circumferentially and axially and mitigates confounding effects due to cannulation, clamping/ligation, forced pressurization, and complete surgical separation of the aorta from surrounding connective tissue.

As with all animal models, the elastase murine model does not represent fully the spatial and temporal evolution of human aneurysms (i.e., acute onset at a predetermined location with evolution over the course of weeks in mice compared to an insidious onset and evolution over years in humans). Nevertheless, since the time of onset of human AAAs is almost always

unknown, and any given lesion (or region within a single lesion) may exist within a wide range of states of progression (i.e., from quiescent to actively dilating), we considered multi-region data from lesions at multiple states of remodeling. Indeed, evidence suggests that human AAAs may undergo intermittent periods of rapid expansion¹² and may possess heterogeneous regions of matrix turnover and potentially destabilizing internal dissections of bioactive thrombus²⁵ that could create a wide range of spatial and temporal states of remodeling. For more details regarding various animal models of aortic aneurysms and their similarities and differences to human disease, we direct the interested reader to two recent reviews.^{15,19}

While this study was not specifically powered to compare regional evolutions of properties, some general observations were apparent. First, elastolysis initiated the lesion while collagen production lagged the loss of elastin. This finding is consistent with previous growth and remodeling models wherein increased stress due to elastolysis takes time to stimulate collagen production as a means of attempting to restore homeostatic stress.^{22,23} Diameter also increased over time, consistent with continued turnover of extracellular matrix. On average, by 2 to 4 weeks, aortic diameter increased more than 50% relative to control, which is the generally accepted clinical definition of an aneurysm. Larger (but likely more homogeneous) lesions could be created by excising free the entire circumference of the aorta before elastase treatment, as reported previously.^{4,13}

Diameter and Wall Thickness

While diameter classically has been the parameter of greatest interest to clinicians, consideration of multiple regions and remodeling times did not reveal a clearly predictive correlation between increasing diameter and either collagen or elastin integrity even though normalized collagen increased and elastin grade decreased in general as expected (Fig. 6), particularly at the anterior apex (Fig. 3). Circumferential Green strain (20–140 mmHg) at the anterior wall of the apex and shoulder appeared better correlated with local diameter; however, any potential correlation was lost when considering the undamaged posterior regions. Thus, diameter alone is non-ideal for assigning biomechanical properties in circumferentially heterogeneous clinical aneurysms with regionally unique extents of damage and rupture-risk.

On the other hand, Fig. 5 suggests that wall thickness may be a good predictor of collagen content in most cases, though further experimentation into correlating fractions of collagen would be valuable. Importantly, collagen content would be overestimated

for the three potential outliers in Fig. 5, if using a linear correlation and measured wall thickness. This error could significantly underestimate the predicted stress (and thus rupture-risk) if these values were used to create a patient-specific model of wall stress. Notably, the points in question had some of the highest adventitial cell grades (two grade 4 and one grade 3), suggesting that the high cellularity led to increased thickness independent of collagen. Note that both of the grade 4 samples were 1 week post-elastase. Importantly, these acutely damaged areas would be most vulnerable to an underestimation of stress despite having a potentially high risk of rupture. We suggest, therefore, that using wall thickness as a proxy for collagen must include a correction for increased adventitial cellularity in areas of recent damage and active remodeling. This caveat is equally relevant for all current models of wall stress that use imaging-derived wall thickness. Future use of novel cell-targeted imaging agents may make non-invasive quantification of these cellular infiltrates possible, which could include invading inflammatory cells and mesenchymal cells that have been recruited as part of the healing response. Exact identification of these cells and their lineage would be useful in future studies.

Circumferential Green Strain

Circumferential Green strain varied greatly for low values of normalized collagen (Fig. 8). Similarly, collagen content was distributed over a wide range for low values of circumferential strain. Thus, this strain may not be a good predictor of total collagen content when considering diverse states of remodeling. Interestingly, while this relationship might be captured by an exponential curve (i.e., a steep reduction of strain immediately after elastolysis, followed by an increase in collagen *via* growth and remodeling), the three data points between 0.2 and 0.3 Green strain and 200–400% collagen would represent samples where collagen would be underestimated for a given strain. Of note, all three points represented regions with intermediate elastin loss (grade 2). The significance of this observation is indeterminate in this study, and further investigation into the potential relationship between the degree/rapidity of elastolysis, the number of functional SMCs, and the rate of collagen production is recommended. Additionally, this study was limited to assessment of total collagen content by area fraction using Masson's trichrome staining. More specific immunohistochemical staining or biochemical methods targeting other collagen metrics such as collagen I:III ratios, cross-linking, fiber diameters, and orientations could add new insights to the complex relationship between strain and collagen in future studies.

While diameter and thickness did not correlate well with elastin grade, local circumferential Green strain (20–140 mmHg) has potential for estimating functional elastin content (see Fig. 7). Recall that this strong correlation was based not simply on total elastin staining, but rather on a combination of the number of lamellae and the presence of damage. Thus, the contribution of elastin to mechanical properties of the aorta depends not only on its mass, but on its arrangement and integrity as well. For example, early signs of elastolysis, including changes in SMC shape and volume, associated with lower circumferential strains than undamaged segments despite equivalent numbers of lamellae. Even a control sample with three healthy elastic lamellae (an anatomic variant) demonstrated lower strain than those with four lamellae (Fig. 7).

Overall, these results suggest that functional elastin is the primary determinant of circumferential Green strain measured from 20 to 140 mmHg. This is not surprising given that elastin has a half-life of 50+ years and is not significantly produced in adulthood^{5,14}; it thus serves as the primary “memory” component of the deformation of the aortic wall during development and disease, and allows significant recoil of the aortic wall upon unloading and high strains upon re-pressurization. Loss of elastin and associated SMCs in the media leaves primarily collagen to bear the load, which is much less extensible and undergoes regular turnover throughout adulthood. As a result, recoil upon unloading of an elastin-deficient aorta (and the resulting strain upon re-pressurization) is reduced.

The statistically significant but weakened correlation of elastin grade to physiologic vs. *in vitro* circumferential strain (Fig. 9) suggests that while functional elastin significantly contributes to physiologic strain, other factors may require elucidation to yield a clinically applicable constitutive relationship. This result likely stems from the nonlinear stress–strain behavior of the aortic wall. That is, as aortic tissue is loaded from an unloaded state, it first exhibits a high initial compliance due to elastin but then transitions to a low compliance regime as collagen fibers engage. The physiologic pressure range lies predominately within this stiffer collagen-dominated regime, particularly for aneurysmal samples that have reduced elastin. Thus, the strain across the physiologic range is limited and masks the full effects of elastin that are evident when loading across sub-physiologic pressures. Attempts to improve the correlation using local diameter, wall thickness, and collagen content were unsuccessful. We expect that other factors not explored in this study, such as collagen cross-linking, orientation, and fiber density/composition, play a role in modulating the

strain at physiological pressures. Future studies in experimental models and human AAAs are recommended for clarification.

Axial Green Strain

A final observation, however, may help with the difficulty of limited physiologic strain, albeit indirectly. Increasing evidence suggests that mechanical changes in the axial (not just circumferential) direction may play important roles in determining overall growth and remodeling of these complex lesions.^{17,24} Similarly, volumetric expansion may be an independent factor from maximum diameter for AAA rupture risk,¹¹ suggesting that axial expansion may be clinically important. Since the infrarenal aorta is axially constrained at the renal arteries proximally and the iliac bifurcation distally, a remodeling lesion that extends axially may unload the aorta axially in the shoulder and neck regions proximal and distal to the AAA. Such an axial unloading (and the resulting anisotropic remodeling) has been predicted computationally,²⁴ and an expected increase in tortuosity that may occur with axial unloading has been observed.¹⁶ Interestingly, 8 of the 10 shoulder samples in this data set had axial strains greater than all other apical and control samples (all with strain >0.01) (Fig. 10). Each of these samples had at least some remaining elastin (grade >0) and were adjacent to apical regions with elastin grades of 0–1. The two shoulder regions below a strain of 0.01 were from one sample where the elastin grade was zero in the shoulder itself and another where the elastin grade at the apex of the same lesion was only 2 (i.e., intermediate damage). These observations suggest, therefore, that lesions with severe elastolysis at the apex induce higher axial strains in the shoulder, assuming at least some elastin remains in the shoulders. Thus, since comparison of axial strains across *in vitro* and physiologic ranges of pressure demonstrated a stronger linear correlation ($\rho_P = 0.93$), physiologic axial strain at the shoulder of the AAA may be a feasible clinical proxy for estimating functional elastin content at the apex of the lesion, provided sufficient resolution exists for obtaining *in vivo* axial strain non-invasively.

CONCLUSIONS

Prediction of rupture risk remains a paramount challenge in the assessment of AAAs. While there is increasing interest in using stress estimations from computational models of patient-specific AAAs to inform clinical decisions, these estimations inherently depend on the assignment of material properties across

a heterogeneously evolving aneurysm. How to assess these microstructure-dependent properties non-invasively remains an open question. From this investigation, we conclude that heterogeneous microstructure cannot be predicted by diameter alone; moreover, although regional wall thickness may be a potential proxy for local collagen content, a correction for regions with increased cellularity should be explored to avoid critically underestimating stress in these potentially vulnerable areas. Correlations with strain appear more promising. While circumferential Green strain correlates strongly with local functional elastin over a broad range of pressures, elucidation of additional microstructural factors will be needed to achieve clinically reliable assignment of patient-specific elastin content. In addition, the effects of regionally heterogeneous flow-induced growth and remodeling stimuli on aortic microstructure must also be considered. Interestingly, physiologic axial strain in the shoulder region of AAAs shows promise as a potential proxy for severity of elastolysis at the apex of the lesion. Follow-up studies using non-invasive imaging modalities should seek to confirm these correlations in experimental models and human AAAs. Finally, novel inverse methods should be developed with the goal of translating patient-specific aortic strains into a set of parameterized constitutive relations needed for understanding and modeling the complex, evolving heterogeneities in AAA biomechanical properties that uniquely determine patient-specific rupture risk.

ACKNOWLEDGMENTS

This work was supported by grants from the American Heart Association (Pre-doctoral fellowship award 13PRE14130007; JSW) and the US National Institutes of Health (R01 HL086418, U01 HL116323; JDH). The authors thank Professor Katia Genovese for her development of the pDIC system and staff at Yale Pathology Tissue Services for histology preparation.

CONFLICT OF INTEREST

The authors declare no conflicts of interest.

HUMAN AND ANIMAL STUDIES

All animal surgeries and post-operative care were approved by and performed according to the policies of the Yale Institutional Animal Care and Use Com-

mittee. No human studies were carried out for this study.

REFERENCES

- ¹Anjum, A., R. von Allmen, R. Greenhalgh, and J. T. Powell. Explaining the decrease in mortality from abdominal aortic aneurysm rupture. *Br J Surg* 99:637–645, 2012.
- ²Bersi, M. R., C. Bellini, P. Di Achille, J. D. Humphrey, K. Genovese, and S. Avril. Novel methodology for characterizing regional variations in the material properties of murine aortas. *J Biomech Eng* 2016:138, 2016.
- ³Bersi, M. R., M. J. Collins, E. Wilson, and J. D. Humphrey. Disparate changes in the mechanical properties of murine carotid arteries and aorta in response to chronic infusion of angiotensin-II. *Int J Adv Eng Sci Appl Math* 4(4):228–240, 2012.
- ⁴Bhamidipati, C. M., G. S. Mehta, G. Lu, C. W. Moehle, C. Barbery, P. D. DiMusto, A. Laser, I. L. Kron, G. R. Upchurch, and G. Ailawadi. Development of a novel murine model of aortic aneurysms using peri-adventitial elastase. *Surgery* 152:238–246, 2012.
- ⁵Campbell, E., J. Pierce, S. Endicott, and S. Shapiro. Evaluation of extracellular matrix turnover. Methods and results for normal human lung parenchymal elastin. *Chest* 99:49S, 1991.
- ⁶Genovese, K. A video-optical system for time-resolved whole-body measurement on vascular segments. *Opt Lasers Eng* 49:995–1008, 2009.
- ⁷Genovese, K., M. J. Collins, Y. U. Lee, and J. D. Humphrey. Regional finite strains in an angiotensin-II induced mouse model of abdominal aortic aneurysms. *Cardiovasc Eng Technol* 3:194–202, 2012.
- ⁸Genovese, K., Y. U. Lee, and J. D. Humphrey. Novel optical system for in vitro quantification of full surface strain fields in small arteries: I. Theory and design. *Comput Methods Biomech Biomed Eng* 14:213–225, 2011.
- ⁹Genovese, K., Y. U. Lee, and J. D. Humphrey. Novel optical system for in vitro quantification of full surface strain fields in small arteries: II. Correction for refraction and illustrative results. *Comput Methods Biomech Biomed Eng* 14:227–237, 2011.
- ¹⁰Genovese, K., Y. U. Lee, A. Y. Lee, and J. D. Humphrey. An improved panoramic digital image correlation method for vascular strain analysis and material characterization. *J Mech Behav Biomed Mater* 27:132–142, 2013.
- ¹¹Kontopodis, N., E. Metaxa, Y. Papaharilaou, E. Georgakarakos, D. Tsetis, and C. V. Ioannou. Value of volume measurements in evaluating abdominal aortic aneurysms growth rate and need for surgical treatment. *Eur J Radiol* 83:1051–1056, 2014.
- ¹²Kurvers, H., F. J. Veith, E. C. Lipsitz, T. Ohki, N. J. Gargiulo, N. S. Cayne, W. D. Suggs, C. H. Timaran, G. Y. Kwon, S. J. Rhee, and C. Santiago. Discontinuous, staccato growth of abdominal aortic aneurysms. *J Am Coll Surg* 199:709–715, 2004.
- ¹³Laser, A., G. Lu, A. Ghosh, K. Roelofs, B. McEvoy, P. DiMusto, C. M. Bhamidipati, G. Su, Y. Zhao, C. L. Lau, G. Ailawadi, J. L. Eliason, P. K. Henke, and G. R. Upchurch. Differential gender- and species-specific formation of aneurysms using a novel method of inducing abdominal aortic aneurysms. *J Surg Res* 178:1038–1045, 2012.

- ¹⁴Lefevre, M., and R. B. Rucker. Aorta elastin turnover in normal and hypercholesterolemic Japanese quail. *Biochim Biophys Acta* 630:519–529, 1980.
- ¹⁵Lysgaard Poulsen, J., J. Stubbe, and J. S. Lindholt. Animal models used to explore abdominal aortic aneurysms: a systematic review. *Eur J Vasc Endovasc Surg* 52:487–499, 2016.
- ¹⁶Park, C. S., J. I. Park, K. G. Kim, C. N. Cho, B. U. Ahn, and H. J. Jae. A quantitative evaluation of abdominal aorta aneurysm by CT images. *Technol Health Care* 23:37–45, 2015.
- ¹⁷Raaz, U., A. M. Zöllner, I. N. Schellinger, R. Toh, F. Nakagami, M. Brandt, F. C. Emrich, Y. Kayama, S. Eken, M. Adam, L. Maegdefessel, T. Hertel, A. Deng, A. Jagger, M. Buerke, R. L. Dalman, J. M. Spin, E. Kuhl, and P. S. Tsao. Segmental aortic stiffening contributes to experimental abdominal aortic aneurysm development. *Circulation* 131:1783–1795, 2015.
- ¹⁸Raghavan, M. L., J. Kratzberg, E. M. Castro de Tolosa, M. M. Hanaoka, P. Walker, and E. S. da Silva. Regional distribution of wall thickness and failure properties of human abdominal aortic aneurysm. *J Biomech* 39:3010–3016, 2006.
- ¹⁹Sénémaud, J., G. Caligiuri, H. Etienne, S. Delbosc, J. B. Michel, and R. Coscas. Translational relevance and recent advances of animal models of abdominal aortic aneurysm. *Arterioscler Thromb Vasc Biol* 37:401–410, 2017.
- ²⁰Thubrikar, M. J., M. Labrosse, F. Robicsek, J. Al-Soudi, and B. Fowler. Mechanical properties of abdominal aortic aneurysm wall. *J Med Eng Technol* 25:133–142, 2001.
- ²¹Vallabhaneni, S. R., G. L. Gilling-Smith, T. V. How, S. D. Carter, J. A. Brennan, and P. L. Harris. Heterogeneity of tensile strength and matrix metalloproteinase activity in the wall of abdominal aortic aneurysms. *J Endovasc Ther* 11:494–502, 2004.
- ²²Wilson, J. S., S. Baek, and J. D. Humphrey. Importance of initial aortic properties on the evolving regional anisotropy, stiffness and wall thickness of human abdominal aortic aneurysms. *J R Soc Interface* 9:2047–2058, 2012.
- ²³Wilson, J.S., S. Baek, and J.D. Humphrey. Parametric study of effects of collagen turnover on the natural history of abdominal aortic aneurysms. In: Proceedings of the Royal Society A 2013, p. 469.
- ²⁴Wilson, J. S., and J. D. Humphrey. Evolving anisotropy and degree of elastolytic insult in abdominal aortic aneurysms: potential clinical relevance? *J Biomech* 47:2995–3002, 2014.
- ²⁵Wilson, J. S., L. Virag, P. Di Achille, I. Karsaj, and J. D. Humphrey. Biochemomechanics of intraluminal thrombus in abdominal aortic aneurysms. *J Biomech Eng* 135:021011, 2013.